Chitosan scaffold as an alternative adsorbent for the removal of hazardous food dyes from aqueous solutions

CrossMark

V.M. Esquerdo [a], T.R.S. Cadaval Jr. [a], G.L. Dotto [b], L.A.A. Pinto [a,*]

[a] Unit Operation Laboratory, School of Chemistry and Food, Federal University of Rio Grande, FURG, Engenheiro Alfredo Huch Street, 475, 96201-900 Rio Grande, RS, Brazil
[b] Chemical Engineering Department, Federal University of Santa Maria, UFSM, Roraima Avenue, 1000, 97105-900 Santa Maria, RS, Brazil

ABSTRACT

Hypothesis: The dye adsorption with chitosan is considered an eco-friendly alternative technology in relation to the existing water treatment technologies. However, the application of chitosan for dyes removal is limited, due to its low surface area and porosity. Then we prepared a chitosan scaffold with a megaporous structure as an alternative adsorbent to remove food dyes from solutions.
Experiments: The chitosan scaffold was characterized by infrared spectroscopy, scanning electron microscopy and structural characteristics. The potential of chitosan scaffold to remove five food dyes from solutions was investigated by equilibrium isotherms and thermodynamic study. The scaffold–dyes interactions were elucidated, and desorption studies were carried out.
Findings: The chitosan scaffold presented pore sizes from 50 to 200 μm, porosity of $92.2 \pm 1.2\%$ and specific surface area of $1135 \pm 2 \text{ m}^2 \text{ g}^{-1}$. The two-step Langmuir model was suitable to represent the equilibrium data. The adsorption was spontaneous, favorable, exothermic and enthalpy-controlled process. Electrostatic interactions occurred between chitosan scaffold and dyes. Desorption was possible with NaOH solution (0.10 mol L^{-1}). The chitosan megaporous scaffold showed good structural characteristics and high adsorption capacities ($788–3316 \text{ mg g}^{-1}$).

© 2014 Elsevier Inc. All rights reserved.

1. Introduction

Chitosan is a cationic biopolymer obtained from chitin deacetylation, which makes up the exoskeletons of crustaceans, such as, shrimps and crabs [1]. Due to characteristics such as, biocompatibility, hydrophilicity and biodegradability, chitosan is used in a wide range of applications, including dye removal from liquid effluents [2]. In this field, the advantages of chitosan are non-toxicity, cost-effectiveness, high efficiency (because the amino and hydroxyl groups on chitosan chains serve as binding sites) and capacity to development of complex materials [3]. Generally, for dye removal, chitosan is used in powder form [3–5], however, in this form, chitosan has disadvantages, such as, low values of specific surface area and void fraction [6]. These characteristics hinder the diffusion of the dyes within the chitosan structure, limiting the access to the internal adsorption sites [7,8]. These limitations can be overcome by obtaining a chitosan scaffold with high porosity and adsorption capacity.

Dyes are used in the food industries to improve the sensorial, technological and commercial aspects of the products, but, they can cause serious damages to the human health and environment [9,10]. An amount of these dyes is lost during the manufacturing process, resulting in colored effluents, which are characterized by pH values ranging from 5.5 to 8.5 and temperature of approximately 30 °C [2,11]. The inadequate disposal of dye containing effluents into the environment causes limitation in the water re-oxygenation ability, reducing the photosynthetic activity of aquatic systems, causing acute and chronic toxicities [2,11,12]. Furthermore, the regulations worldwide regarding the discharge of dye containing effluents are more stringent [11]. In this way, the search for technologies to remove dyes from aqueous solutions has received attention in literature [13].

Several techniques have been used to treat colored effluents, for example oxidation [14], photocatalytic degradation [15], coagulation [16], adsorption [17] and others [2]. Among these, adsorption is a good way to treat colored effluents, because of its advantages compared to the conventional methods, especially from the economical and environmental viewpoints [12,18,19]. In the adsorption field, many adsorbents have been employed to remove dyes from aqueous solutions, including silica microspheres [17], activated carbon [18], agricultural solid wastes [19] and chitosan

* Corresponding author. Fax: +55 53 3233 8745.
  E-mail addresses: nessafurg@gmail.com (V.M. Esquerdo), titoeq@gmail.com (T.R.S. Cadaval Jr.), guilherme_dotto@yahoo.com.br (G.L. Dotto), dqmpinto@furg.br (L.A.A. Pinto).

[20]. It is recognized in the literature that the adsorption onto chitosan is an alternative technology to remove dyes from aqueous media [3,4]. The adsorption capacity of chitosan depends on its physical structural parameters, such as, crystallinity, surface area, porosity and particle size [2]. In this way, the development of chitosan scaffold with high values of specific surface area and porosity is an alternative to improve its characteristics as adsorbent.

This study aimed to obtain and characterize a chitosan scaffold in order to apply in the adsorption of hazardous food dyes. The chitosan scaffold was prepared and characterized by Fourier transform infrared spectroscopy (FT-IR), scanning electron microscopy (SEM), and structural characteristics. The potential of chitosan scaffold to remove the hazardous food dyes was investigated by equilibrium isotherms and thermodynamic parameters (ΔG^0, ΔH^0, ΔS^0), at different temperatures (298–328 K). Analyses of Fourier transform infrared spectroscopy, scanning electron microscopy, X-ray mapping and color were performed before and after the adsorption process to elucidate the interactions chitosan scaffold–dyes. Desorption studies were carried out to verify the reuse of the chitosan scaffold.

2. Material and methods

2.1. Preparation and characterization of chitosan scaffold

Chitosan in powder form (molecular weight 150 ± 3 kDa, deacetylation degree of 85 ± 1% and mean diameter of 72 ± 3 μm) was obtained from shrimp (*Penaeus brasiliensis*) wastes, according to the procedures presented in our previous works [21,22]. The chitosan megaporous scaffold was prepared as follows: chitosan sample (2.0 g) was dissolved in 100 mL of 1.0% acetic acid solution under magnetic stirring for 24 h at room temperature. Afterwards, the chitosan solution was homogenized at 10,000 rpm for 5 min (Dremel, 1100-01, Brazil), and it was maintained at 193 K during 48 h in an ultra-freezer (Indrel, IULT 90-D, Brazil). Finally, it was carried out in freeze drying at 219 K for 48 h under vacuum of 44 mmHg (Liobras, L108, Brazil). The sample was conditioned in a desiccator prior to the characterization and use. The mentioned procedures were based in preliminary tests and literature [23,24].

The functional groups on chitosan scaffold were identified by Fourier transform infrared spectroscopy (FT-IR) (Prestige, 21210045, Japan) [25]. Scanning electron microscopy (SEM) (Jeol, JSM-6610LV, Japan) was used to evaluate the textural characteristics [26]. The specific surface area (A_S) was determined by a volumetric adsorption analyzer (Quantachrome Instruments, New Win 2, USA) using the Bennett, Emmet and Teller (BET) method [27]. The solid density (ρ_s) was obtained from the literature [28] and the apparent density (ρ_p) was estimated by mass:volume ratio in an electronic balance (Marte, AY220, Brazil). The porosity (ε_p) and the pore volume (V_p) were calculated by Eqs. (1) and (2), respectively [27]:

$$\varepsilon_p = 1 - \frac{\rho_p}{\rho_s} \qquad (1)$$

$$V_p = \frac{1}{\rho_p} - \frac{1}{\rho_s} \qquad (2)$$

where ρ_p is apparent density (kg m^{-3}) and ρ_s is solid density (kg m^{-3}).

2.2. Food dyes
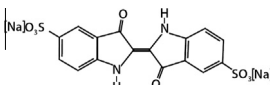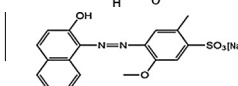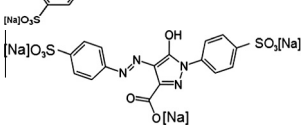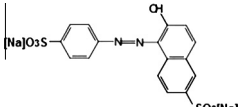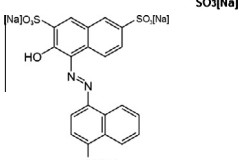
In this work, five food dyes were used: FD&C blue 2, FD&C red 40, FD&C yellow 5, FD&C yellow 6 and Food red 2. These dyes were supplied by Duas Rodas Ind. (Brazil), with purity higher than 85%, and used without further purification. The characteristics of the food dyes are shown in Table 1. All other reagents were of analytical grade and the experiments were performed with distilled water.

2.3. Equilibrium experiments

The equilibrium isotherms were obtained for the five dyes, at different temperatures (298, 313 and 328 K), and all other experimental conditions were determined by preliminary tests and literature [3,12,29]. Firstly, dye stock solutions (1.0 g L^{-1}) were prepared with distilled water, and the pH was adjusted to 6.0 (this pH is usual for colored effluents [11]) through the buffer disodium phosphate/citric acid solution (0.1 mol L^{-1}), which did not present

Table 1
Characteristics of the food dyes.

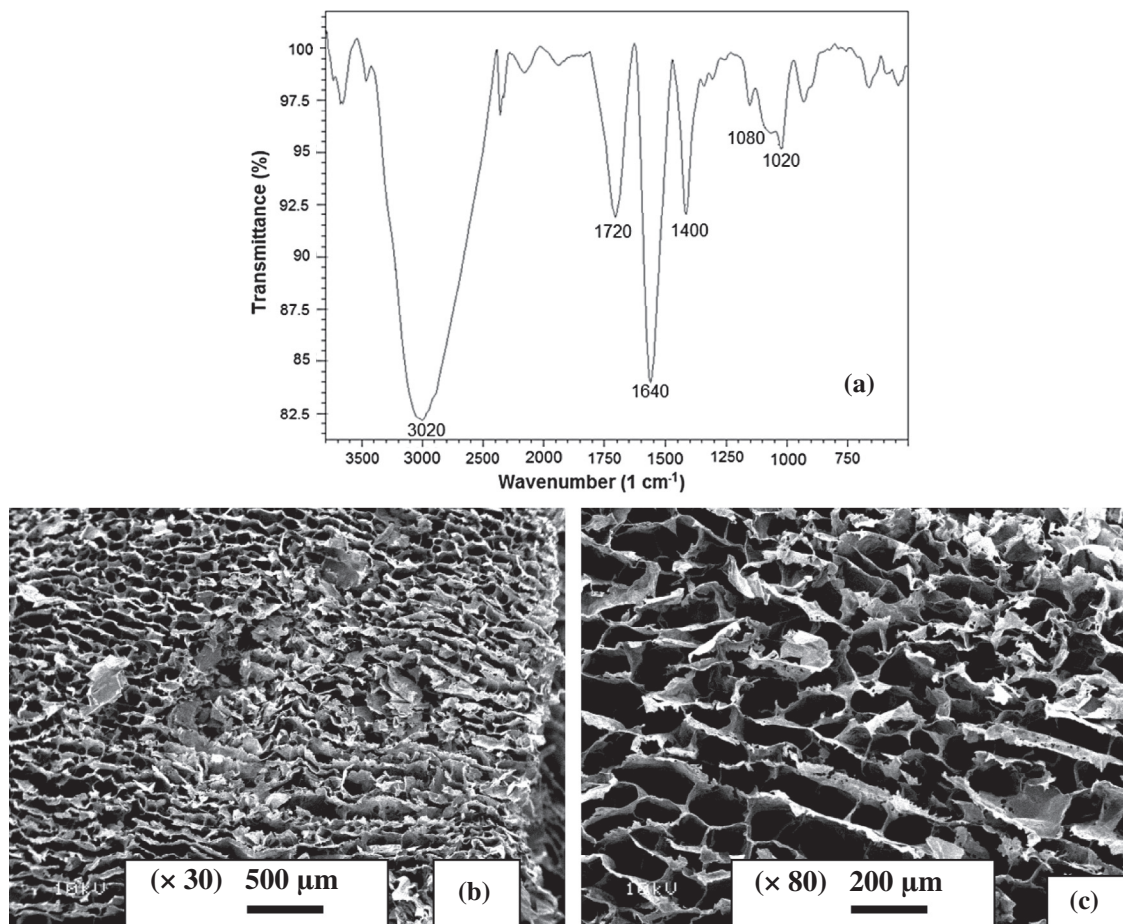| Food dye	Color index (C.I.)	Wavelength (λ_{max}) (nm)	Molecular weight (g mol^{-1})	Chemical structure
FD&C blue 2	73,015	610	466.3	
FD&C red 40	16,045	500	496.4	
FD&C yellow 5	19,140	425	534.4	
FD&C yellow 6	15,985	480	452.4	
Food red 2	16,185	521	604.5	

Fig. 1. Characteristics of chitosan scaffold: (a) FT-IR spectrum, (b) SEM image (×30) and (c) SEM image (×80).

interaction with the dyes [29]. Afterward, the experiments were carried out by dilution of the stock solutions. Chitosan scaffold (250 mg L^{-1}) was added in the dye solutions with different initial concentrations (100, 200, 300, 400, 500, 600 and 700 mg L^{-1}). These solutions were agitated at 100 rpm using a thermostated type Wagner agitator (Fanem, 315 SE, Brazil). The equilibrium was considered attained when the dye concentration in the liquid did not present difference between three consecutive measures. The equilibrium concentration was determined by spectrophotometry (Biospectro, SP-22, Brazil). The experiments were carried out in replicate (three times for each experiment) and blanks were performed. The equilibrium adsorption capacity (q_e) was determined by Eq. (3):

$$q_e = \frac{V(C_0 - C_e)}{m} \tag{3}$$

where C_0 is the initial dye concentration in liquid (mg L^{-1}), C_e is the equilibrium dye concentration in liquid (mg L^{-1}), m is the amount of adsorbent (g) and V is the volume of solution (L).

2.4. Two-step Langmuir model

A two-step Langmuir model was used to represent the equilibrium isotherms in the adsorption of food dyes onto chitosan scaffold. This model is obtained from the sum of two Langmuir-type isotherms, with the assumption that sterically or energetically heterogeneous adsorption sites exist on the adsorbent. Each step on the curve represents different (or identical) types of adsorption sites with different affinities (or availabilities). The two-step Langmuir model is shown by Eq. (4) [30]:

$$q_e = \sum_{i=1}^{n} \frac{q_{mi} k_{Li}(C_e - C_c)}{1 + k_{Li} C_e} \tag{4}$$

where q_{mi} is the maximum adsorption capacity for the step 'i' (mg g^{-1}), k_{Li} is the Langmuir constant (L mg^{-1}) for the step 'i' and C_c is the critical concentration (the critical concentration is the remaining dye concentration in the liquid phase after the first step of saturation) (mg L^{-1}); the subscript 'i' is relative to each step. In this work, 'i' = 2, so, Eq. (4) becomes Eqs. (5) and (6), for the first and second steps, respectively [31]:

$$q_e = \frac{q_{m1} k_{L1} C_e}{1 + k_{L1} C_e} \tag{5}$$

$$q_e = \frac{q_{m1} k_{L1} C_e}{1 + k_{L1} C_e} + \frac{q_{m2} k_{L2}(C_e - C_c)}{1 + k_{L2} C_e} \tag{6}$$

In order to obtain the total adsorption capacity (q_m), the Eq. (7) can be used [31]:

$$q_m = q_{m1} + q_{m2} \tag{7}$$

The parameters were obtained by non-linear regression using the Simplex/Quasi-Newton estimation method [32]. The fit quality was measured by coefficient of determination (R^2) and average relative error (ARE) [13]. The calculations were realized using the Statistic software (Statistic 6.0, Statsoft, USA).

2.5. Thermodynamic calculations

The thermodynamic parameters, such as, Gibbs free energy change (ΔG^0, kJ mol^{-1}), enthalpy change, (ΔH^0, kJ mol^{-1}) and
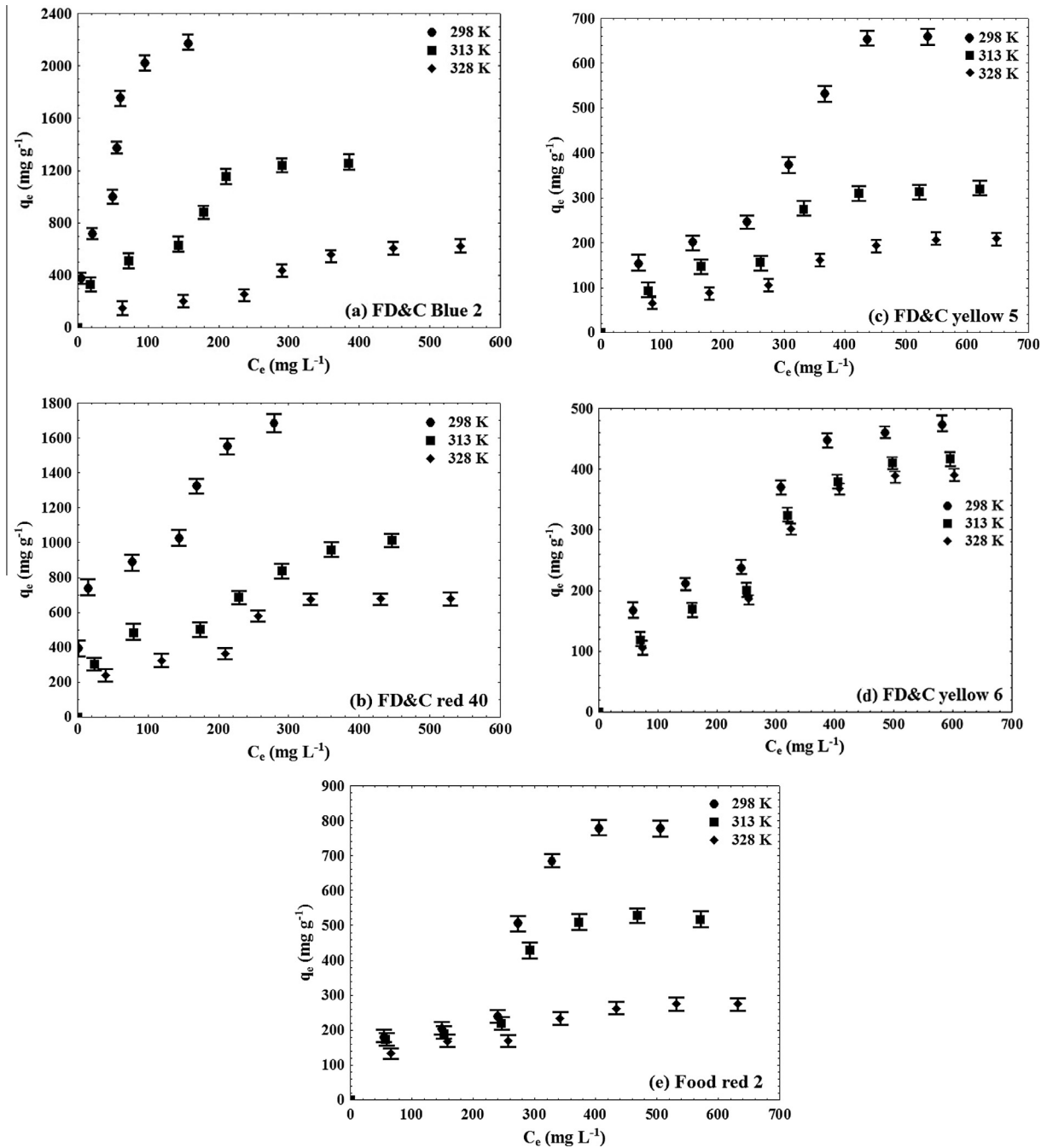
Fig. 2. Equilibrium isotherms of food dyes adsorption onto chitosan scaffold: (a) FD&C blue 2, (b) FD&C red 40, (c) FD&C yellow 5, (d) FD&C yellow 6 and (e) Food red 2. (● 298 K; ■ 313 K; ♦ 328 K).

entropy change (ΔS^0, kJ mol^{-1} K^{-1}) were estimated by Eqs. (8)–(10) [33–35]:

$$\Delta G^0 = \Delta H^0 - T\Delta S^0 \tag{8}$$

$$\Delta G^0 = -RT \ln(\rho_w K_D) \tag{9}$$

$$\ln(\rho_w K_D) = -\frac{\Delta H^0}{RT} + \frac{\Delta S^0}{R} \tag{10}$$

where R is the universal gas constant (kJ mol^{-1} K^{-1}), T is the temperature (K), ρ_w is the water density (g L^{-1}) and K_D is the thermodynamic equilibrium constant (L g^{-1}). The values of K_D were obtained by plotting q_e/C_e versus q_e and extrapolating q_e to zero [34,36].

2.6. Interactions analyses

In order to elucidate the possible interactions chitosan scaffold–dyes, analyses of Fourier transform infrared spectroscopy, scanning electron microscopy, X-ray mapping and color were performed before and after the adsorption process. FT-IR and SEM were carried out in the same way of Section 2.2 [25,26]. X-ray mappings were carried out to identify the presence of the dyes (by mean of sulfur) on the chitosan scaffold after the adsorption process (Jeol, JSM-6610LV, Japan) [26]. The color parameters were determined before and after adsorption process by Minolta system (Minolta Corporation, CR-300, Japan). Color was measured from three-dimensional color diagram (L^*, a^*, b^*), were L^* is lightness, a^* is chromaticity

Table 2
Two-step Langmuir parameters for the adsorption of food dyes onto chitosan scaffold.

	FD&C blue 2			FD&C red 40			FD&C yellow 5			FD&C yellow 6			Food red 2		
	298 K	313 K	328 K	298 K	313 K	328 K	298 K	313 K	328 K	298 K	313 K	328 K	298 K	313 K	328 K
Step I															
q_{m1} (mg g^{-1})	1260	705	342	870	579	407	304	225	144	274	272	271	253	226	192
k_{L1} (L mg^{-1})	0.073	0.045	0.011	0.639	0.049	0.036	0.016	0.001	0.009	0.027	0.011	0.009	0.052	0.043	0.036
R^2	0.995	0.994	0.995	0.992	0.996	0.999	0.994	0.993	0.999	0.999	0.999	0.998	0.991	0.992	0.998
ARE (%)	3.6	3.1	2.9	3.5	2.5	1.1	2.9	3.3	1.0	1.0	0.8	2.1	3.3	2.9	1.4
Step II															
q_{m2} (mg g^{-1})	1772	1190	847	2446	869	755	774	242	203	514	360	351	1299	759	199
k_{L2} (L mg^{-1})	0.022	0.043	0.026	0.003	0.019	0.133	0.062	0.035	0.009	0.008	0.046	0.123	0.034	0.039	0.226
C_C (mg L^{-1})	49	142	236	77	174	209	238	261	274	240	250	253	240	245	257
R^2	0.956	0.991	0.981	0.971	0.988	0.955	0.954	0.987	0.983	0.958	0.988	0.982	0.966	0.958	0.974
ARE (%)	5.3	1.6	4.0	2.0	1.4	4.3	6.4	5.4	4.5	6.1	1.4	5.2	6.5	8.6	1.1
q_m (mg g^{-1})	3032	1895	1189	3316	1448	1162	1078	467	347	788	632	622	1552	985	391

from green ($-$) to red ($+$); b^* is chromaticity from blue ($-$) to yellow ($+$). Hue angle (H_{ab}) and the total color variation (ΔE_{ab}^*) were calculated by Eqs. (11) and (12) [37]:

$$H_{ab} = \tan^{-1}\left(\frac{b^*}{a^*}\right) \quad (11)$$

$$\Delta E_{ab}^* = \sqrt{(\Delta L^*)^2 + (\Delta a^*)^2 + (\Delta b^*)^2} \quad (12)$$

where $\Delta L^* = L_{sample}^* - L_{reference}^*$, $\Delta a^* = a_{sample}^* - a_{reference}^*$ and $\Delta b^* = b_{sample}^* - b_{reference}^*$. The reference values are relative to the chitosan scaffold before the adsorption process, while, the sample values are relative to the chitosan scaffold adsorbed with the dyes.

2.7. Desorption analysis

In order to verify the possible reuse of the chitosan scaffold adsorption–desorption cycles were carried out using 100 mL of eluent solution and 250 mg L^{-1} of chitosan scaffold loaded with the dyes. Solutions of NaCl (0.05–0.50 mol L^{-1}) and NaOH (0.05–0.50 mol^{-1}) were tested as eluents.

3. Results and discussion

3.1. Chitosan scaffold characteristics

The characteristics of chitosan scaffold are shown in Fig. 1.
In the FT-IR spectrum (Fig. 1(a)), the following bands can be observed: 3020, 1720, 1640, 1400, 1080, 1020 cm^{-1}. The broad band centered at 3020 cm^{-1} is relative to the O—H and N—H stretchings. The C=O vibration of amide band I can be observed at 1720 cm^{-1}.

The band at 1550 cm^{-1} can be assigned to the C—N stretchings of amide. The C—O—H and H—C—H links may be observed at 1400 cm^{-1}. The C—N of amine and the C—O links can be identified at 1080 and 1020 cm^{-1}, respectively. In brief, the FT-IR spectrum confirmed that the NH$_2$ and OH typical groups of the chitosan are present in its megaporous scaffold. These groups are potential sites for dyes adsorption [3,38].

In Fig. 1(b) and (c) it was observed that the chitosan scaffold presented a megaporous structure with pores sizes from 50 to 200 μm. This confirms that the chitosan scaffold obtained in this work is a megaporous material. Furthermore, the values of specific surface area (A_s), porosity (ε_p) and pore volume (V_p) were respectively, 1135 ± 2 m^2 g^{-1}, 92.2 ± 1.2% and 7.9 × 10^{-3} ± 1.9 × 10^{-3} m^3 kg^{-1}. These values are highest compared with others chitosan based materials, for example, chitosan powder (A_s = 4.2 m^2 g^{-1} V_p = 9.5 × 10^{-6} m^3 kg^{-1}) [28], chitosan beads (A_s = 30–40 m^2 g^{-1}), chitosan flakes (A_s = 4–6 m^2 g^{-1}) [39], chitosan hydrogel beads (ε_p = 85%) [40] and chitosan–graphene mesostructure (A_s = 603.2 m^2 g^{-1}) [41]. These characteristics are particularly important for adsorption purposes, because allows the access of the large dye molecules (see Table 1) into the internal adsorption sites [3]. Based on the above mentioned, it can be inferred that the scaffold obtained in this work improved the structural characteristics of chitosan for adsorption purposes.

3.2. Equilibrium adsorption studies

The equilibrium curves for all dyes studied are shown in Fig. 2, and it can be seen that the equilibrium isotherms were of a type IV [42].

Table 3
Thermodynamic parameters for the adsorption of food dyes onto chitosan scaffold.

Food dye	Temperature (K)	K_D (L g^{-1})[a]	ΔG^0 (kJ mol^{-1})[a]	ΔH^0 (kJ mol^{-1})[a]	ΔS^0 (kJ mol^{-1} K^{-1})[a]	$T\Delta S^0$ (kJ mol^{-1})[a]
FD&C blue 2	298	60.61 ± 0.23	−27.26 ± 0.02			−12.52 ± 0.01
	313	33.07 ± 0.45	−27.05 ± 0.01	−40.01 ± 0.73	−0.042 ± 0.001	−13.15 ± 0.01
	328	13.92 ± 0.21	−25.97 ± 0.04			−13.78 ± 0.01
FD&C red 40	298	72.18 ± 0.69	−27.69 ± 0.03			−15.79 ± 0.01
	313	26.25 ± 0.56	−26.45 ± 0.01	−43.28 ± 0.41	−0.053 ± 0.001	−16.59 ± 0.01
	328	14.85 ± 0.28	−26.14 ± 0.01			−17.38 ± 0.01
FD&C yellow 5	298	4.85 ± 0.07	−21.01 ± 0.06			−13.41 ± 0.01
	313	1.98 ± 0.11	−19.75 ± 0.01	−34.35 ± 0.52	−0.045 ± 0.001	−14.08 ± 0.01
	328	1.39 ± 0.08	−19.69 ± 0.01			−14.76 ± 0.01
FD&C yellow 6	298	7.33 ± 0.98	−22.03 ± 0.09			−10.13 ± 0.01
	313	2.99 ± 0.01	−20.79 ± 0.17	−32.06 ± 0.55	−0.034 ± 0.001	−10.64 ± 0.01
	328	2.29 ± 0.02	−21.05 ± 0.51			−11.15 ± 0.01
Food red 2	298	11.14 ± 0.34	−23.07 ± 0.01			−1.79 ± 0.01
	313	7.01 ± 0.27	−23.01 ± 0.01	−24.91 ± 0.32	−0.006 ± 0.001	−1.88 ± 0.01
	328	4.49 ± 0.37	−22.88 ± 0.08			−1.97 ± 0.01

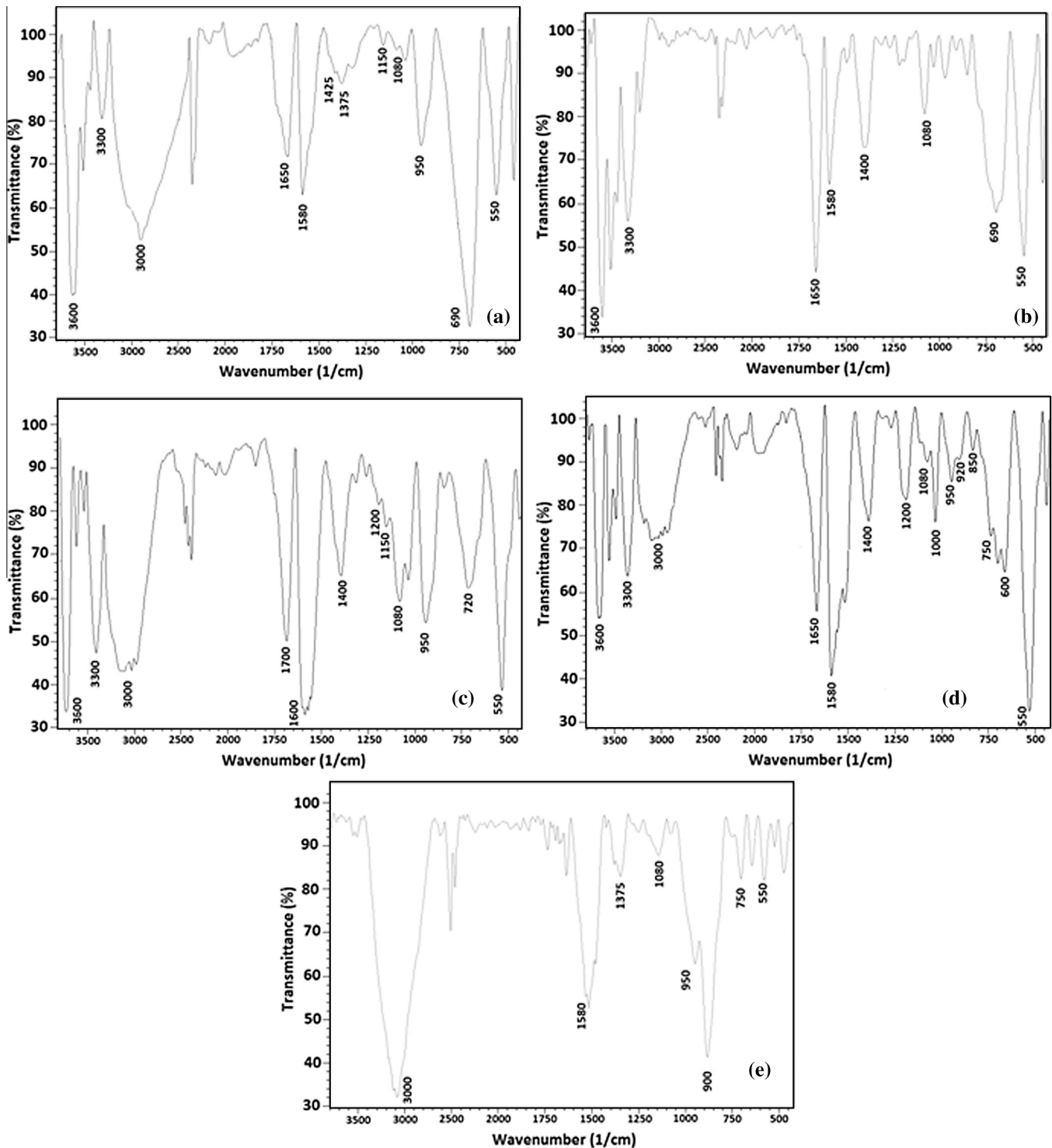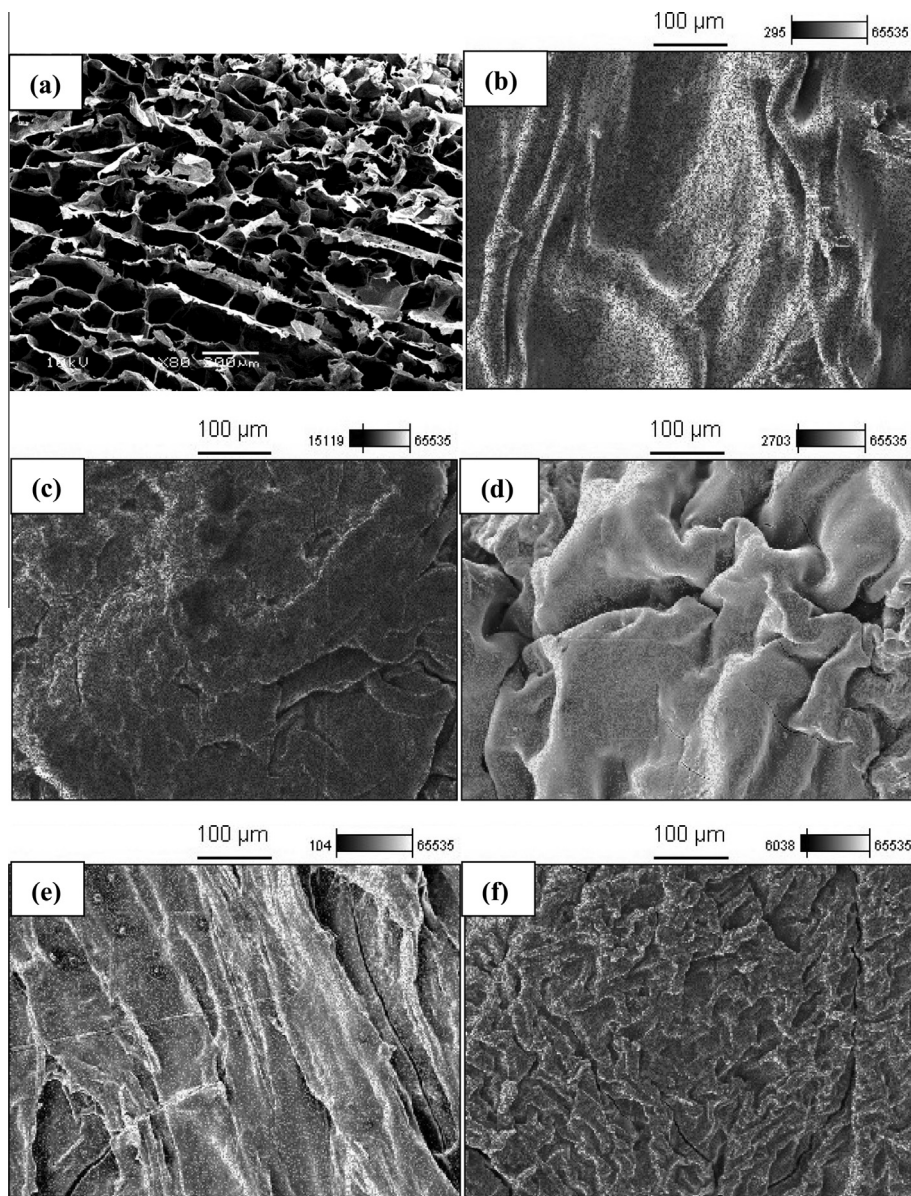[a] Mean ± standard deviation (n = 3).

Fig. 3. FT-IR spectrum of chitosan scaffold after the adsorption process: (a) FD&C blue 2, (b) FD&C red 40, (c) FD&C yellow 5, (d) FD&C yellow 6 and (e) Food red 2.

An isotherm curve of type IV proposes the formation of two layers on a plane surface or on the wall of a pore very much wider than the molecular diameter of the adsorbate [7]. The type IV curves are consistent for the system chitosan scaffold–food dyes, since the scaffold has pore sizes (50–200 μm) very higher than the molecular size of the dyes (13.9–18.0 Å). Similar curves were found in the biosorption of lead (II) from aqueous solutions by solid wastes [31].

In Fig. 2 the adsorption capacities were favored by the temperature decrease, and the maximum values were attained at 298 K.

This can be occurred because the temperature increase leads to an increase in the solubility of the dyes [3], so, the interactions forces between the food dyes and the water become stronger than the forces between the dyes and the chitosan scaffold. Similar behavior was found in the adsorption of food dyes onto chitosan films [29].

In order to represent the equilibrium curves, the two-step Langmuir model was fitted with the experimental data, and the results are shown in Table 2. The high values of the coefficient of determination ($R^2 > 0.95$) and the low values of the average relative error

Fig. 4. SEM images and sulfur X-ray mappings for the chitosan scaffold (a) before adsorption process, (b) adsorbed with FD&C blue 2, (c) adsorbed with FD&C red 40, (d) adsorbed with FD&C yellow 5, (e) adsorbed with FD&C yellow 6 and (f) adsorbed with Food red 2.

(ARE < 10%) (Table 2) show that the two-step Langmuir model is suitable to represent the equilibrium curves in the adsorption of food dyes on chitosan scaffold. Based on the interaction mechanism chitosan–anionic dyes [3,5,20,28,38] (and also proved in Section 3.4) and in the good fit of the two-step Langmuir model, it can be inferred that: firstly, at low adsorbate concentrations, the dye molecules occupied the amino groups on the plane surface of the pores (which are more available from the physical viewpoint), forming a monolayer; then, at highest concentrations, the dye molecules occupied the amino groups on the pore walls (which are less available due steric restrictions), characterizing the multilayer adsorption.

Table 2 shows that the values of q_{m1}, q_{m2} and q_m were increased as a function of the temperature decrease, confirming that the adsorption capacity was favored at 298 K. The same trend was found for k_{L1}, indicating a high affinity between scaffold and dyes at lowest temperatures. In addition, the C_C values increased with temperature. This shows that at high temperatures, more dye remained in the solution after the monolayer formation.

The adsorption capacities of some chitosan based materials (powder, film, flakes, beads, chitosan hydrogel beads, chitosan–zinc oxide nanoparticles, chitosan–CTAB modified bentonites and chitosan–polyaniline/ZnO hybrid composites) are from 71.4 to 1026.0 mg g^{-1} [1,4,6,20,29,39,40,43]. Based on these results, it can be affirmed that the chitosan scaffold obtained in this work is a good adsorbent to remove food dyes from aqueous solutions.

3.3. Thermodynamic parameters

The adsorption thermodynamic behavior was evaluated by the estimation of K_D, ΔG^0, ΔH^0 and ΔS^0, and these values are shown in Table 3. It was found that the K_D values increased with the temperature decrease. This confirms that the adsorption of food dyes on chitosan scaffold was favored at 298 K. The negative values of ΔG^0 indicated that the adsorption was a spontaneous and favorable process. For all studied dyes, negative values of ΔH^0 were verified (Table 3), demonstrating that the adsorption of food dyes on chitosan scaffold was an exothermic process. Furthermore, from

Table 4
Color parameters of chitosan scaffold before and after the adsorption process.

Chitosan scaffold	L[A]	a[A]	b[A]	H_{ab} (°)[A]	ΔE_{ab}[A]
Before adsorption	86.84 ± 0.22	1.02 ± 0.05	13.15 ± 0.34	85.55 ± 0.08	0
Adsorbed with FD&C blue 2	36.02 ± 2.36	−5.57 ± 0.58	2.84 ± 0.21	236.96 ± 2.63	55.66 ± 7.16
Adsorbed with FD&C red 40	20.01 ± 0.28	34.60 ± 0.50	12.65 ± 0.38	20.08 ± 0.29	74.79 ± 0.06
Adsorbed with FD&C yellow 5	62.37 ± 0.74	22.79 ± 0.62	78.76 ± 0.87	73.86 ± 0.44	73.32 ± 0.58
Adsorbed with FD&C yellow 6	38.02 ± 3.04	43.68 ± 1.32	38.76 ± 2.43	41.58 ± 1.83	69.71 ± 1.70
Adsorbed with Food red 2	15.29 ± 2.39	14.94 ± 2.59	2.84 ± 0.21	10.75 ± 1.60	73.61 ± 5.71

[A] Mean ± standard deviation (n = 3).

the magnitude of ΔH^0 it is possible to infer about the interactions adsorbent–adsorbate; the physisorption, such as, van der Waals interaction is usually lower than 20 kJ mol^{-1}, the electrostatic interaction ranges from 20 to 80 kJ mol^{-1}, and the chemisorption bond strengths can be from 80 to 450 kJ mol^{-1} [44,45]. In this way, it can be inferred that electrostatic interactions can have occurred between the food dyes and the chitosan scaffold. The negative values of ΔS^0 show that the randomness decreases at the solid–solution interface during the adsorption. Comparing the values of ΔH^0 and $T\Delta S^0$ (Table 3) it can be verified that the adsorption of food dyes on chitosan scaffold was an enthalpy-controlled process. Similar thermodynamic behavior was found by Dotto et al. [29] in the adsorption of food dyes onto chitosan films, and Piccin et al. [28] in the adsorption of FD&C red 40 onto chitosan powder.

3.4. Interactions chitosan scaffold–food dyes

The interactions chitosan scaffold–food dyes were investigate by FT-IR spectrums (Fig. 3), SEM and X-ray mappings (Fig. 4) and color parameters (Table 4).

In the FT-IR spectrums of chitosan scaffold after adsorption (Fig. 3), some modifications were verified in relation to the spectrum before adsorption (see Fig. 1(a)). The main modifications occurred from 3600 to 3000 cm^{-1} (N—H stretching) and from 1580 to 1520 cm^{-1} (C—N stretching), indicating that the chitosan amino groups were involved in the interactions with the food dyes. Furthermore, asymmetric and symmetric O=S=O stretchings appeared, respectively, at 1425–1375 cm^{-1} and 1200–1150 cm^{-1}. This shows that the sulfonated groups of the dyes were involved in the interactions with chitosan scaffold.

Fig. 4(a) shows the porous network of the chitosan scaffold before adsorption process (as discussed in Section 3.1). After the adsorption process (Fig. 4(b–f)), the pores disappeared and the surface was smoothed. Furthermore, the X-ray mappings after the adsorption process revealed the presence of sulfur along the chitosan scaffold surface. These results confirm that the food dyes were densely and homogeneously adhered on the chitosan scaffold.

Table 4 shows a decrease in L^* values, indicating that the chitosan scaffold darkened after the adsorption process. The H_{ab} values found a yellowness coloration for chitosan scaffold before adsorption process. However, after adsorption, the scaffold acquired the characteristic color of each dye. The ΔE_{ab}^* values showed a strong color variation in the chitosan scaffold adsorbed with the food dyes. These color parameters (L^*, H_{ab}, ΔE_{ab}^*) show that the chitosan scaffold was strongly colored during the adsorption, showing its high affinity with the food dyes.

Based on the FT-IR (Fig. 3), SEM and X-ray mappings (Fig. 4), color parameters (Table 4) and thermodynamic parameters (Tables 2 and 3), it can be proposed that electrostatic interactions occurred between the chitosan scaffold (protonated amino groups) and the food dyes (sulfonated groups). This interaction mechanism was also verified in other researches, which used chitosan based materials as adsorbents [3,5,20,38,41].

3.5. Desorption analysis

It was verified that 0.10 mol L^{-1} of NaOH solution was the more suitable eluent. This result confirms the electrostatic interaction between the chitosan scaffold and the dyes (Section 3.4), since this interaction was corrupted with the NaOH solution [13]. All dyes were desorbed from chitosan scaffold at only 5 min. The reuse was possible for two cycles maintaining the same adsorption capacity.

4. Conclusion

A chitosan scaffold was prepared and characterized, and its potential to remove five hazardous food dyes from aqueous solutions was evaluated by equilibrium studies, thermodynamic parameters, interaction analyses and desorption tests. The chitosan scaffold showed suitable structural characteristics for adsorption purposes, with high values of pore size, porosity and specific surface area. The experimental equilibrium data were well fitted by two-step Langmuir model, and the total adsorption capacities ranged from 788 to 3316 mg g^{-1}, at 298 K. The thermodynamic parameters showed that the adsorption of the food dyes onto chitosan scaffold was a spontaneous, favorable, exothermic and enthalpy-controlled process. Based on the magnitude of ΔH^0, FT-IR, SEM and X-ray mappings, it was concluded that electrostatic interactions occurred between the chitosan scaffold and the food dyes. The desorption tests showed that chitosan scaffold can be used for two cycles maintaining the same adsorption capacity.

References

[1] R. Salehi, M. Arami, N.M. Mahmoodi, H. Bahrami, S. Khorramfar, Colloids Surf. B: Biointerfaces 80 (2010) 86–93.
[2] A. Srinivasan, T. Viraraghavan, J. Environ. Manage. 91 (2010) 1915–1929.
[3] G. Crini, P.M. Badot, Polym. Sci. 33 (2008) 399–447.
[4] G.L. Dotto, L.A.A. Pinto, Carbohydr. Polym. 84 (2011) 231–238.
[5] N.M. Mahmoodi, R. Salehi, M. Arami, H. Bahrami, Desalination 267 (2011) 64–72.
[6] P. Kannusamy, T. Sivalingam, Colloids Surf. B: Biointerfaces 108 (2013) 229–238.
[7] D.M. Ruthven, Principles of Adsorption and Adsorption Processes, John Wiley & Sons, New York, 1984.
[8] W.J. Weber Jr., F.A. Di Giano, Process Dynamics in Environmental Systems, John Wiley & Sons, New York, 1995.
[9] S. Sharma, R.P. Goyal, G. Chakravarty, A. Sharma, Exp. Toxicol. Pathol. 60 (2008) 51–57.

[10] FDA, US Food and Drugs Administration. Color additives. <http://www.fda.gov/ForIndustry/Coloradditives/ColoradditivesinSpecificProductsInFood/default.htm>, 2013.

[11] C. Hessel, C. Allegre, M. Maisseu, F. Charbit, P. Moulin, J. Environ. Manage. 83 (2007) 171–180.

[12] V.K. Gupta, Suhas, J. Environ. Manage. 90 (2009) 2313–2342.

[13] N.F. Cardoso, E.C. Lima, B. Royer, M.V. Bach, G.L. Dotto, L.A.A. Pinto, T. Calvete, J. Hazard. Mater. 241–242 (2012) 146–153.

[14] C. Wang, Y. Zhang, L. Yu, Z.H. Zhang, H. Sun, J. Hazard. Mater. 260 (2013) 851–859.

[15] T.A. Saleh, V.K. Gupta, J. Colloid Interface Sci. 371 (2012) 101–106.

[16] D. Morshedi, Z. Mohammadi, M.M.A. Boojar, F. Aliakbari, Colloids Surf. B: Biointerfaces 112 (2013) 245–254.

[17] F. Wang, Y. Tang, B. Zhang, B. Chen, Y. Wang, J. Colloid Interface Sci. 386 (2012) 129–134.

[18] A. Demirbas, J. Hazard. Mater. 167 (2009) 1–9.

[19] M.A.M. Salleh, D.K. Mahmoud, W.A.W.A. Karim, A. Idris, Desalination 280 (2011) 1–13.

[20] G.L. Dotto, L.A.A. Pinto, J. Hazard. Mater. 187 (2011) 164–170.

[21] R.F. Weska, J.M. Moura, L.M. Batista, J. Rizzi, L.A.A. Pinto, J. Food Eng. 80 (2007) 749–753.

[22] G.L. Dotto, V.C. Souza, J.M. Moura, C.M. Moura, L.A.A. Pinto, Drying Technol. 29 (2011) 1784–1791.

[23] E. Landi, F. Valentini, A. Tampieri, Acta Biomater. 4 (2008) 1620–1626.

[24] B. Yang, X.Y. Li, S. Shi, X.Y. Kong, G. Guo, M. Huang, F. Luo, Y.Q. Wei, X. Zhao, Z.Y. Qian, Carbohydr. Polym. 80 (2010) 860–865.

[25] R.M. Silverstein, F.X. Webster, D.J. Kiemle, Spectrometric identification of organic compounds, Wiley, New York, 2007.

[26] J.I. Goldstein, D.E. Newbury, P. Echil, D.C. Joy, A.D. Romig Jr., C.E. Lyman, C. Fiori, E. Lifshin, Scanning Electron Microscopy and X-ray Microanalysis, Plenum Press, New York, 1992.

[27] R. Leyva-Ramos, R. Ocampo-Perez, J. Mendoza-Barron, Chem. Eng. J. 183 (2012) 141–151.

[28] J.S. Piccin, G.L. Dotto, M.L.G. Vieira, L.A.A. Pinto, J. Chem. Eng. Data 56 (2011) 3759–3765.

[29] G.L. Dotto, J.M. Moura, T.R.S. Cadaval, L.A.A. Pinto, Chem. Eng. J. 214 (2013) 8–16.

[30] L.N. Konda, I. Czinkota, G. Füleky, G. Morovjan, J. Agric. Food Chem. 50 (2002) 7326–7331.

[31] G. Blázquez, M. Calero, F. Hernáinz, G. Tenorio, M.A. Martín-Lara, Chem. Eng. J. 160 (2010) 615–622.

[32] L. Tolner, Appl. Ecol. Environ. Res. 6 (2008) 111–119.

[33] S.K. Milonjic, J. Serb. Chem. Soc. 72 (2007) 1363–1367.

[34] Y. Liu, J. Chem. Eng. Data 54 (2009) 1981–1985.

[35] X. Zhou, H. Liu, J. Hao, Ads. Sci. Technol. 30 (2012) 647–649.

[36] J.S. Piccin, G.L. Dotto, L.A.A. Pinto, Braz. J. Chem. Eng. 28 (2011) 295–304.

[37] D.K. Youn, H.K. No, W. Prinyawiwatkul, Food Sci. Technol. 42 (2009) 1553–1556.

[38] W.S. Wan Ngah, L.C. Teong, M.A.K.M. Hanafiah, Carbohydr. Polym. 83 (2011) 1446–1456.

[39] F.C. Wu, R.L. Tseng, R.S. Juang, J. Hazard. Mater. B 73 (2000) 63–75.

[40] S. Chatterjee, D.S. Lee, M.W. Lee, S.H. Woo, Bioresour. Technol. 100 (2009) 2803–2809.

[41] J.S. Cheng, J. Du, W. Zhu, F. Facile synthesis of three-dimensional chitosan–graphene mesostructures for reactive black 5 removal, Carbohydr. Polym. 88 (2012) 61–67.

[42] C.H. Giles, T.H. MacEwan, S.N. Nakhwa, D. Smith, J. Chem. Soc. (1960) 3973–3993.

[43] J. Guo, S. Chen, L. Liu, B. Li, P. Yang, L. Zhang, Y. Feng, J. Colloid Interface Sci. 382 (2012) 61–66.

[44] W.S. Alencar, E.C. Lima, B. Royer, B.D. Santos, T. Calvete, E.A. Silva, C.N. Alves, Sep. Sci. Technol. 47 (2012) 513–526.

[45] F.M. Machado, C.P. Bergmann, E.C. Lima, B. Royer, F.E. Souza, I.M. Jauris, T. Calvete, S.B. Fagan, Phys. Chem. Chem. Phys. 14 (2012) 11139–11153.